Nikola Kostić[1], Ivica Čamagić[1], Aleksandar Sedmak[2], Zijah Burzić[3], Simon Sedmak[4], Goran Mandić[5]

IMPACT TOUGHNESS BEHAVIOUR OF A516 GR. 60 STEEL WELDED JOINTS

UDARNA ŽILAVOST ZAVARENIH SPOJEVA ČELIKA A516 GR. 60

Originalni naučni rad / Original scientific paper
UDK /UDC:
Rad primljen / Paper received:

Adresa autora / Author's address:
1) University of Kosovska Mitrovica, Faculty of Technical Sciences, Serbia
2) University of Belgrade, Faculty of Mechanical Engineering, Serbia
3) Military Technical Institute, Belgrade, Serbia
4) Innovation Center of Faculty of Mechanical Engineering, Belgrade, Serbia
5) Serbian Committee for energy network, Belgrade, Serbia

Keywords
- A516 Gr. 60
- Impact toughness
- Total impact energy
- Welded joint zones

Ključne reči
- A516 Gr. 60
- Udarna žilavost
- UKupna udarna energija
- Zone zavarenog spoja

Izvod

Aanalizirano je ponašanje zavarenih spojeva od konstrukcionog čelika A516 Gr. 60 pri lomu usled udarnog opterećenja. Udarno ispitivanje je urađeno na instrumentiranom Šarpijevom klatnu, na epruvetama sa zarezom u osnovnom metalu (OM), zoni uticaja toplote (ZUT) i metalu šava (MŠ). Ukupna udarna energija je predstavljena kao suma energije nastajanja prsline i energije rasta prsline, kako bi ova analiza bila detaljnija i sveobuhvatnija. Uticaj temperature do -60 °C je takođe analiziran, kako bi se potvrdilo da je čelik A516 Gr. 60 upotrebljiv i na niskim temperaturama.

Abstract

Impact fracture behaviour of welded joints made of A516 Gr. 60 is analysed as a commonly used carbon structural steel for welded structures. Impact testing on Charpy instrumented pendulum is performed using specimens with a notch at positions: the base metal (BM), heat-affected-zone (HAZ), and weld metal (WM). The total impact energy is presented as a sum of energies for crack initiation and crack propagation to make the analysis more sophisticated and comprehensive. The effect of temperature up to -60 °C was also analysed to prove the A516 Gr. 60 steel usability at subzero conditions.

INTRODUCTION

Before using welded joints made of A516 Gr. 60 steel, it is necessary to investigate their properties, with the focus on impact toughness and microstructure to ensure operational safety. Each welded joint region (BM, WM and HAZ) has to be analysed individually, and their impact toughness and transition temperatures to determined and compared to each other, to account for the heterogeneity of a weld, /1-3/. Crack initiation energy and crack propagation energy, as the components of total impact energy should be also considered separately, to provide insight into the nature of fracture which occurred under the effect of impact load at lower temperatures. The main issue here is transition temperature, as the phenomenon which is decisive for the use of a material at lower temperature, as described in couple of recent papers, /4-7/.

MATERIAL AND WELDING PLAN

The A516 Gr.60 is low-alloyed carbon steel, used mainly for pressure vessels, such as spherical tanks and tanks for gas storage. This is largely due to its exceptional mechanical properties at lower temperatures. Its minimum yield stress is 255 MPa and its guaranteed toughness at -40 °C is 41 J. It was manufactured in "Železarna ACRONI", Jesenice, /8-9/. Plates with a thickness of 15 mm were available for experimental tests. The chemical composition of steel A516 Gr. 60 is shown in table 1.

Test specimens were made out of welded joints which were made using the manual arc welding (MAW) process, with EVB Ni electrode as filler material. Nominal mechanical properties and chemical composition for the filler material are shown in tables 2 and 3.

Table 1. Chemical composition of the tested batch of steel A516 Gr. 60, Batch no.: 191314030402, /8/

Measuring number	Element, % wt.									
	C	Si	Mn	P	S	Cu	Al	Cr	Mo	Ni	N
1	0.10	0.19	0.86	0.009	<0,001	0.24	0.036	0.12	0.05	0.16	0.007
2	0.10	0.20	0.86	0.005	<0,001	0.24	0.037	0.12	0.05	0.15	0.004
3	0.10	0.20	0.88	0.007	<0,001	0.25	0.041	0.12	0.05	0.15	0.005
Mean value	0.10	0.20	0.86	0.007	<0,001	0.24	0.038	0.12	0.05	0.15	0.005

Table 2. Chemical composition of filler metal EVB Ni

Filler material	% wt.						
	C	Si	Mn	Ni	P	S	N
EVB Ni	0.07	0.50	1.40	1.1	0.009	0.011	0.012

Table 3. Mechanical properties of filler material EVB Ni

Yield stress $R_{p0,2}$, MPa, min..	Tensile strength Rm, MPa	Elongation A, %, min.	Impact energy, KV, J at -40°C, min.
460	560-720	22	47

Welding plan was defined as follows:

– Root pass - MAW process (denoted as 111 according to EN ISO standards). Filler material was EVB Ni, with a diameter of 2.5 mm.
– Fill passes - MAW process for all passes. Same filler material as the root pass, but with diameters of 2.5 and 3.25 mm.

Schematic display of the preparation and weld geometry is shown in figure 1, whereas the order of welding passes is shown in figure 2.

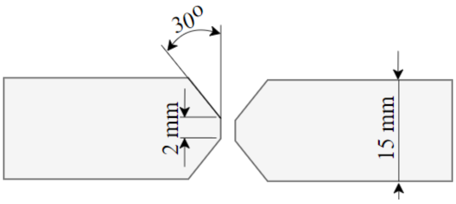

Figure 1. Schematic display of weld geometry and preparation

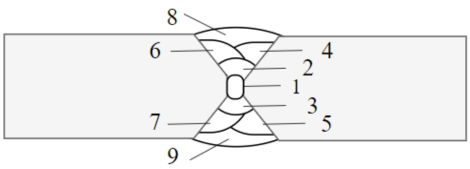

Figure 2. Welding sequence

After the machining of the weld was completed, pre-heating to a temperature of around 120°C was performed.

In order to gain a clearer insight into the micro-structure of the welded joint, with distinctive regions, images were made using a stereo microscope with magnitude 12. Figure 3 shows the weld face, its central section and the weld root. All three regions of the welded joint can be clearly seen in the images - the base metal (BM), heat affected zone with the fusion line (HAZ-FL) and weld metal (WM). Micro-structure of BM, HAZ, FL and WM of the joint is shown in figures 4-7.

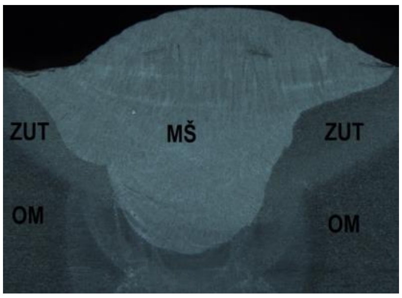

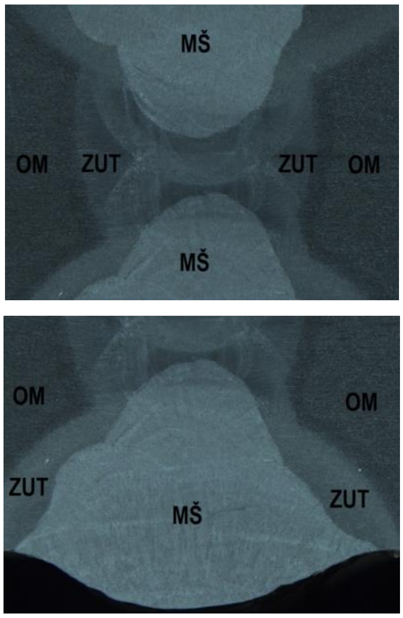

Figure 3. Weld face (top), central section (middle) and root (bottom)

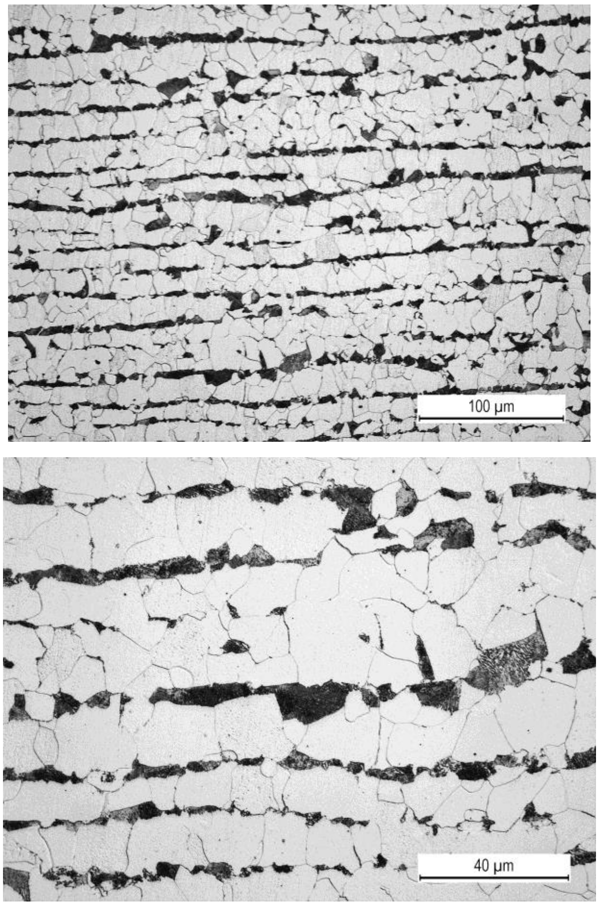

Figure 4. Microstructure of BM (low-alloyed steel A516 Gr. 60)

It can be seen that the BM has a uniformly distributed ferrite-pearlite structure. Ferrite is found in the shape of polygonal crystals, whereas pearlite resembles a compact dark micro-constituent. Weld metal and heat affected zone also have a prominent ferrite-pearlite structure.

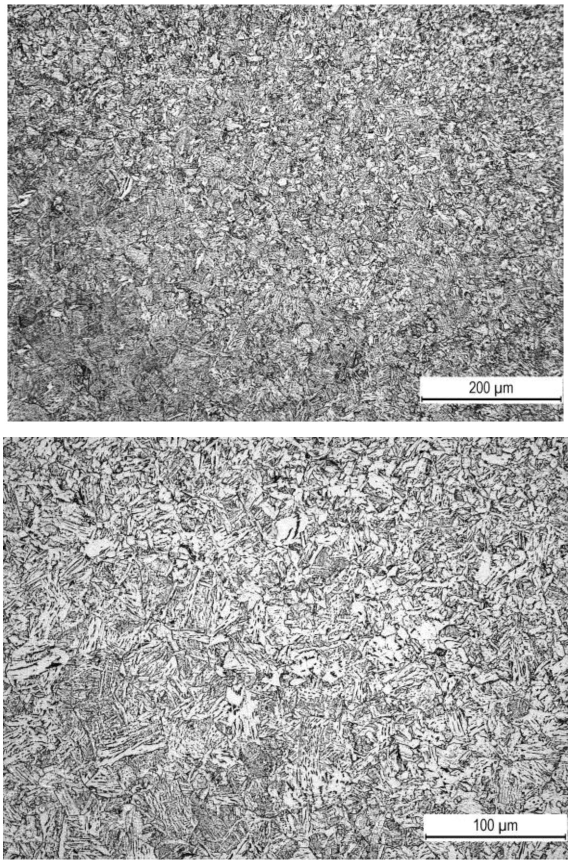

Figure 5. Microstructure of HAZ
(low-alloyed carbon steel A516 Gr. 60)

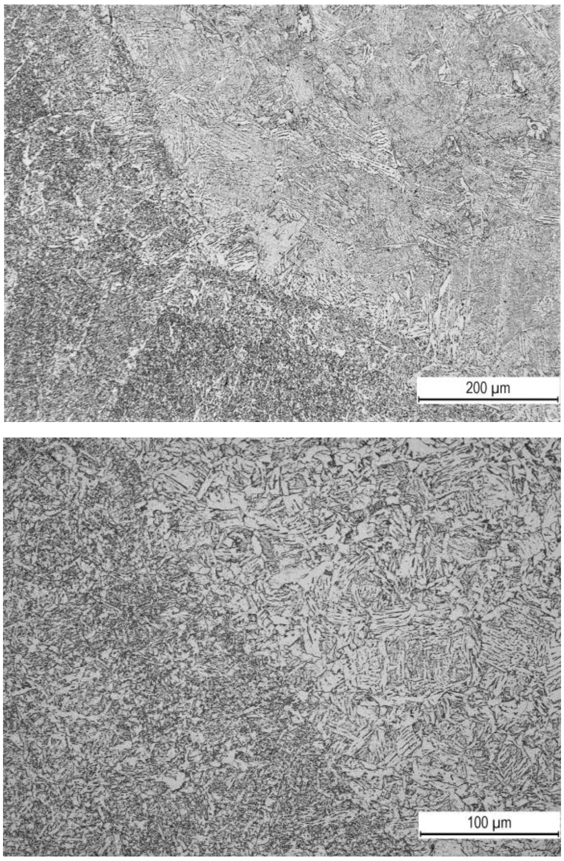

Figure 6. Microstructure of FL (steel A516 Gr. 60)

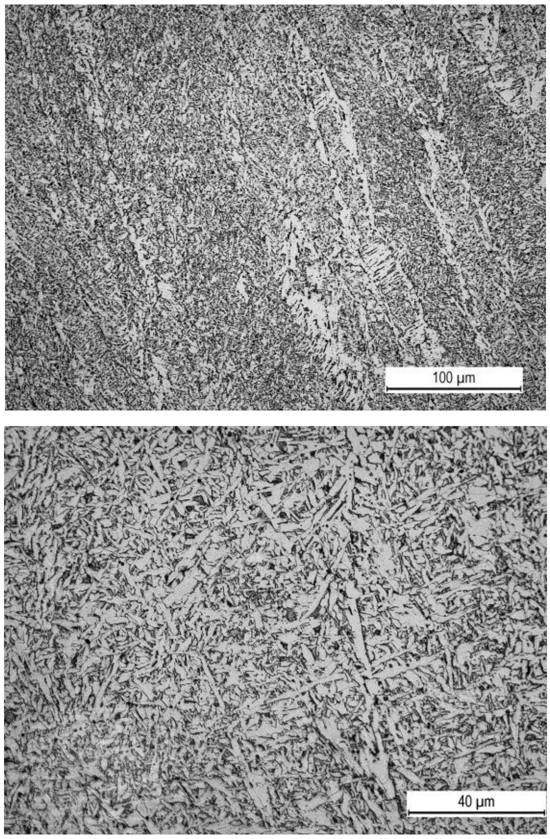

Figure 7. Microstructure of WM (steel A516 Gr. 60)

IMPACT TESTS

Standard Charpy specimens were used for impact tests, /10/, shown in fig. 8. Three groups of specimens were tested, depending on the location of the V-2 notch: Group I - specimens with a notch in the BM, Group II - specimens with notch in the BM and Group III - specimens with notch in the HAZ. Their geometry is shown in figure 9.

In accordance with standard SRPS EN ISO 9016:2022, /11/, specimen type VWT (V: Charpy notch, W: notch in the weld metal, T: notch perpendicular to the thickness) was used for WM and VHT was used for the HAZ (H refers to the notch in the HAZ and other designations are the same as the previous type). The way of positioning the notch in the corresponding welded joint region is shown in figure 9, /11/.

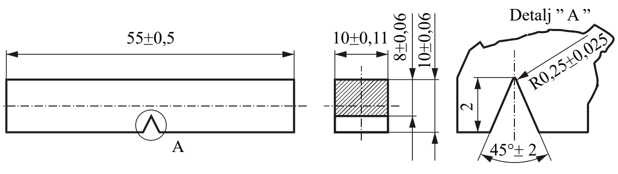

Figure 8. Dimensions of test specimens and the V-2 notch, /11/

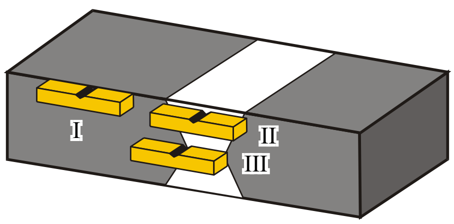

Figure 9. Scheme of notch locations in a welded joint, /11/

However, since the tests were performed using an instrumented Charpy pendulum (in accordance with standard SRPS EN ISO 14556:2023), total impact energy Wt was calculated as the surface area between the force – displacement (deflection) curve and the x axis, following interpretations and analyses, including tabular and graphic representations of test results, will be presented in accordance with the aforementioned standard. Force-displacement curves enable the separation of total impact energy (W_t) into the energy for crack initiation (W_i) and energy for crack propagation (W_p), /12-15/. Testing equipment used in this analysis is shown in figure 10.

Figure 10. Instrumented Charpy pendulum WOLPERT 150/300J

IMPACT TEST RESULTS FOR BM, HAZ AND WM

Results of impact testing of specimens with a notch in the BM are given in table 4. Diagrams force vs. time are shown in figure 11 for BM specimens (and different test temperatures). Results of tests performed on specimens with a notch in the HAZ are presented in the same form, in table 5 and figure 12. For specimens with the notch in the WM, results are given in table 6 and figure 13.

Table 4. Values of impact energy the BM

Specimen designation	Temp. °C	Initiation energy W_i, J	Propagation energy W_p, J	Total impact energy W_t, J
1A	-60	25.5	7.8	33.3
2A		27.5	10.9	38.4
3A		27.1	8.1	35.3
1B	-40	51.3	21.2	72.5
2B		45.1	21.8	66.9
3B		42.4	24.4	68.6
1C	-20	51.3	71.0	122.3
2C		53.9	70.8	124.7
3C		53.9	73.8	127.7
1D	0	62.8	95.4	158.2
2D		64.4	98.6	163.0
3D		60.4	91.1	151.6
1E	20	62.6	139.9	202.5
2E		62	133.4	195.3
3E		65.4	141.7	207.1

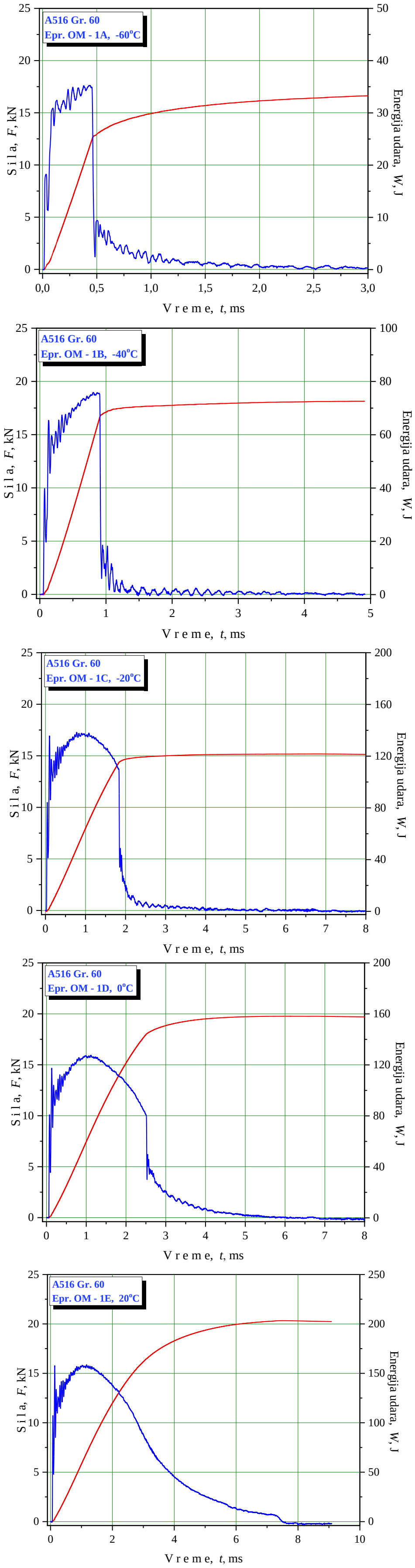

Figure 11. The BM results - force -time diagrams

Table 5. Impact energy for specimens with notch in HAZ

Specimen designation	Temp. °C	Initiation energy W_i, J	Propagation energy W_p, J	Total impact energy W_t, J
ZUT - 1A	-60	28.6	4.3	32.9
ZUT - 2A		26.9	3.5	30.4
ZUT - 3A		28.1	3.4	31.4
ZUT - 1B	-40	45.6	14.3	59.9
ZUT - 2B		41.4	13.8	55.2
ZUT - 3B		47	15.2	62.2
ZUT - 1C	-20	50.3	52.8	103.1
ZUT - 2C		53.7	53.4	107.1
ZUT - 3C		55.6	56.0	111.6
ZUT - 1D	0	59.4	86.5	145.8
ZUT - 2D		60.2	83.4	143.6
ZUT - 3D		60	79.6	139.6
ZUT - 1E	20	57.2	123.0	180.2
ZUT - 2E		60.4	116.5	176.9
ZUT - 3E		61.8	120.4	182.2

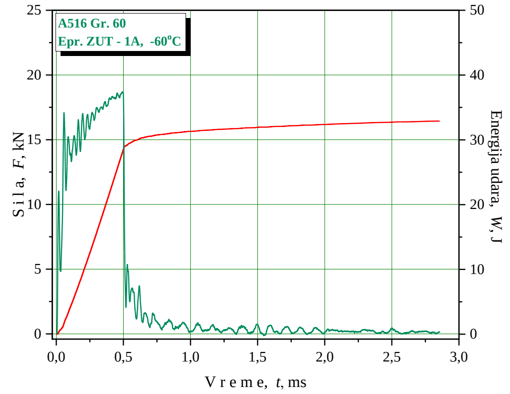

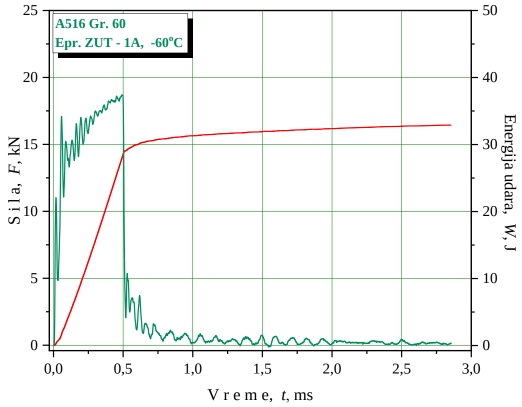

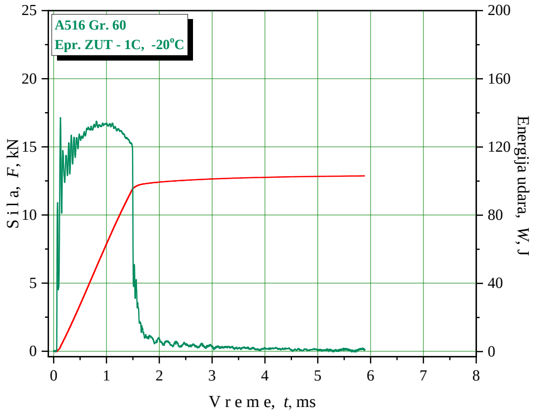

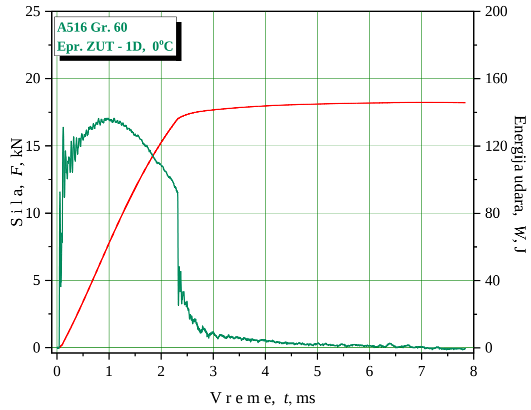

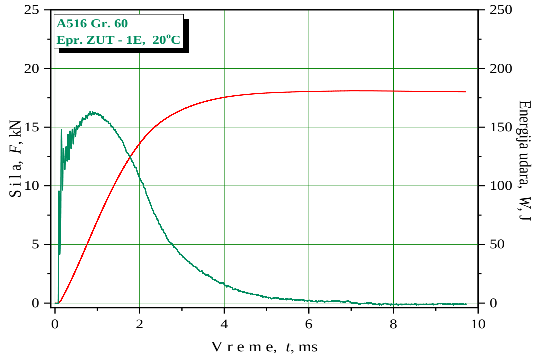

Figure 12. The HAZ results - force -time diagrams

Table 6. Values of impact energy for the WM

Specimen designation	Temp. °C	Initiation energy W_i, J	Propagation energy W_p, J	Total impact energy W_t, J
MŠ - 1A	-60	23.8	5.5	29.3
MŠ - 2A		26.8	3.4	30.2
MŠ - 3A		27.3	1.3	28.6
MŠ - 1B	-40	33.0	11.4	44.4
MŠ - 2B		32.9	10.4	43.3
MŠ - 3B		33.7	12.3	46.0
MŠ - 1C	-20	49.9	37.2	87.1
MŠ - 2C		47.1	30.1	77.2
MŠ - 3C		48.1	34.9	83.0
MŠ - 1D	0	55.6	51.4	107.0
MŠ - 2D		58.9	57.5	116.4
MŠ - 3D		56.7	54.4	111.1
MŠ - 1E	20	65.7	88.9	154.6
MŠ - 2E		62.6	92.7	155.3
MŠ - 3E		65.4	92.2	157.6

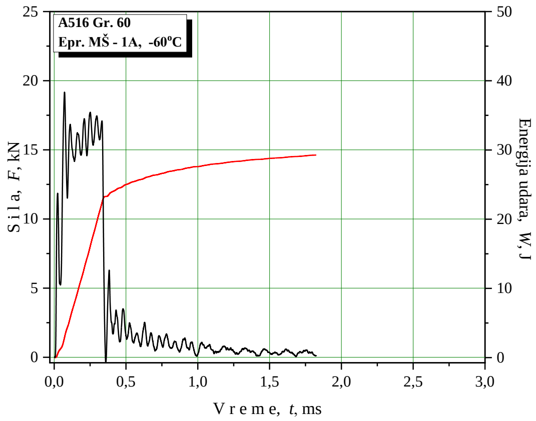

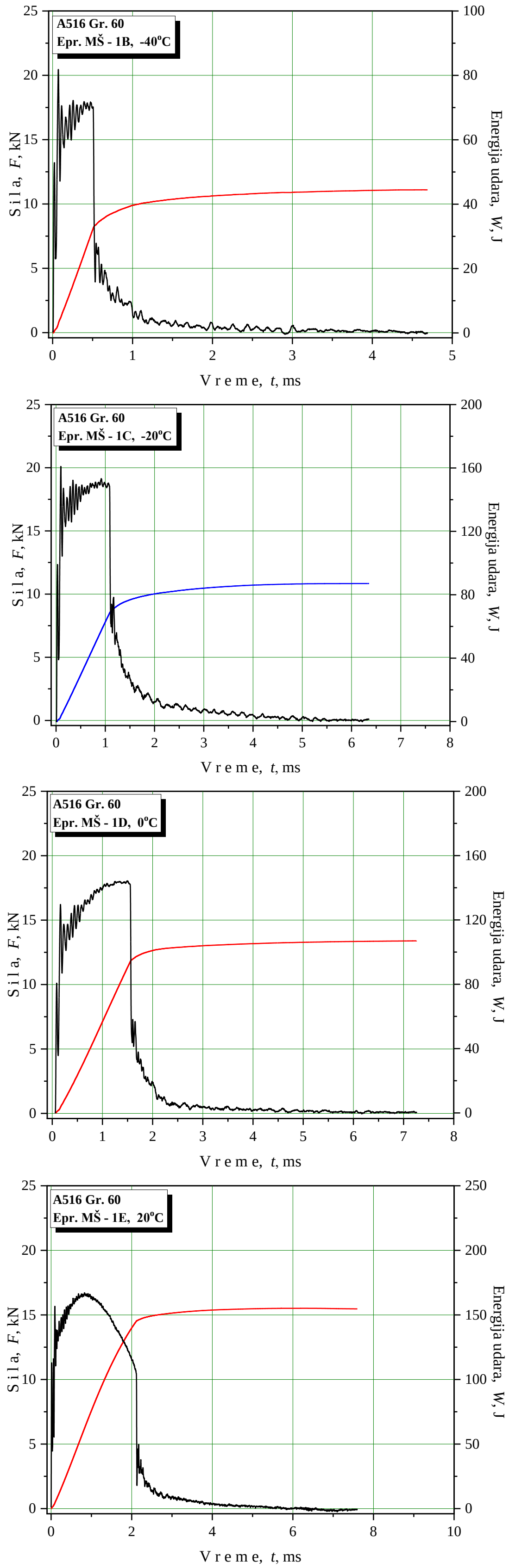

Figure 13. The WM results - force -time diagrams

DISCUSSION

By analysing the obtained curves, it can be seen that they exhibit similar dependence at same temperatures, with only differences being observed in terms of maximum force, F_{max}, deflection s and total impact energy Wt. Dependence of total impact energy, W_t, from temperature and the location of the notch is shown in figure 14. It is well known that the total impact energy W_t depends on:

- Location of notch in terms of welded joint region.
- Testing temperature.

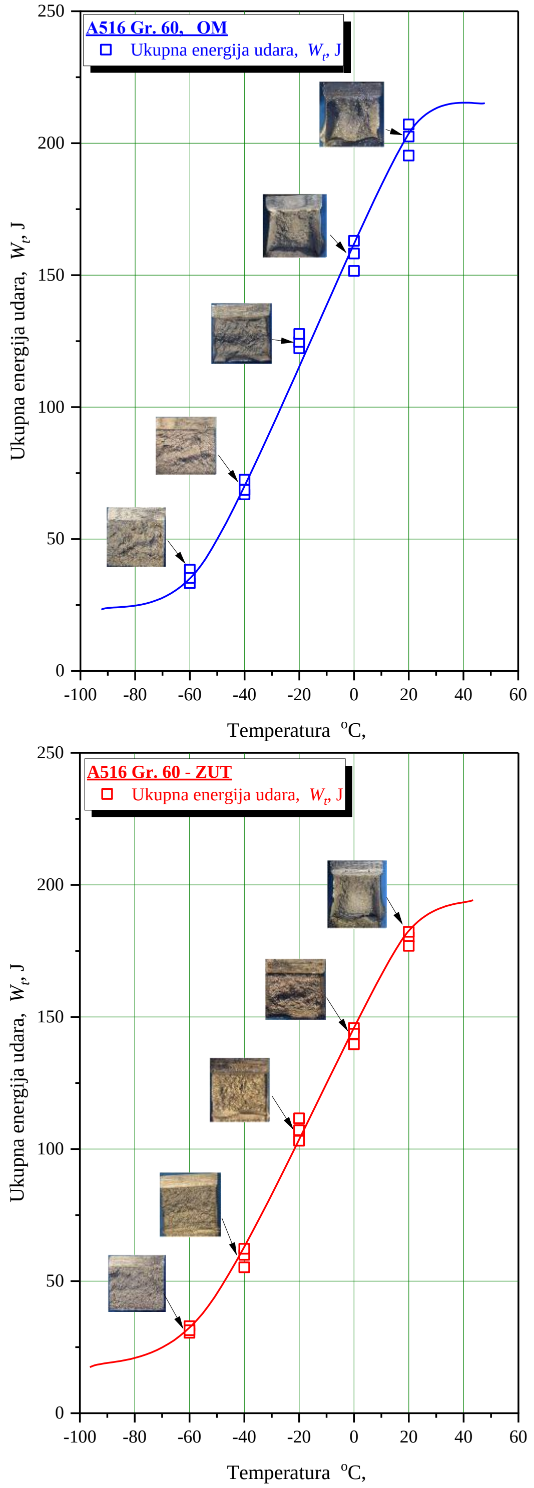

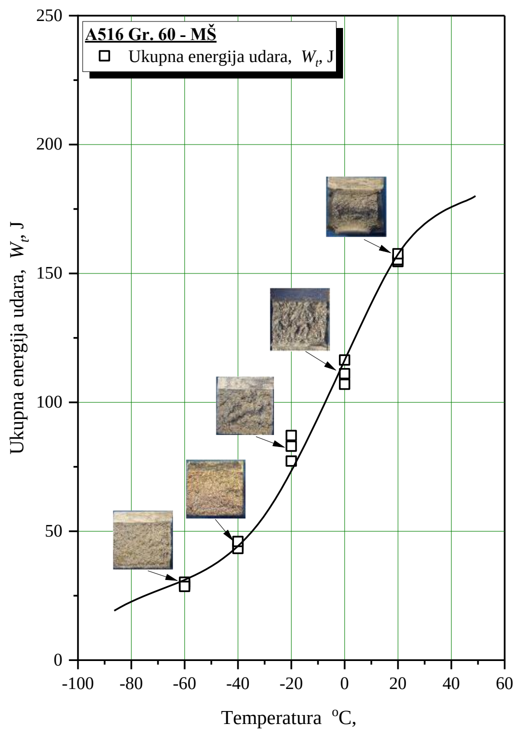

Figure 14. Dependence of total impact energy W_t on temperature

By analysing the effect of notch location on total impact energy (tables 4-6), it can be concluded that the heterogeneity between the microstructures of the BM and WM, results in different mechanical properties and considerably affect total impact energy values. Highest total impact energy values were observed in the BM, whereas specimens with the notch in the HAZ had slightly lower values and the lowest ones were obtained for specimens with the notch in the WM.

However, the highest effect on obtained values of total impact energy and its components (crack initiation and propagation energy), as well as on the failure mechanisms and appearance of fracture surfaces was due to test temperature. Since A516 Gr. 60 steel has a body-centered cubic structure, the effect of temperature is evident. Lowering of temperature favours the initiation of a brittle state and is particularly prominent for this type of steels and welded joints, as typical heterogeneous structure.

Total impact energy, W_t, decreases as the temperature lowers, in a successive manner from room temperature to -60 °C for all welded joint zones (BM - HAZ - WM). Influence of test temperature is most significant for specimens with the notch in the WM, slightly less for HAZ, and the lowest for the BM. More prominent influence of test temperature is closely related to the heterogeneity of WM and HAZ. Weld metal represents previously melted filler material (electrode) and is characterised by a cast structure. Heat affected zone represents the most heterogeneous welded joint region, due to the effect of weld metal melting has on the base metal. In this particular case, due to well defined welding parameters, structural transformation of the BM was somewhat low, hence the obtained total impact energy values were very close to the BM itself.

Total impact energy values obtained for specimens with a V-2 notch in the BM had an average of 202 J. With a decrease in temperature, these values also drop. At 0°C, the mean total impact energy for these specimens was 167 J. Further decrease in temperature (-20°C) resulted in an average of 125 J, whereas test temperature of -40° caused the total impact energy to decrease to an average of 69 J. Finally, at -60°C the mean value of total impact energy was around 36 J.

For the specimens with the V-2 notch in the HAZ, overall values of total impact energy were slightly lower compared to the BM specimens, with an approximate difference of 10%. At room temperature, their mean value was 179 J, whereas at 0°C, this value was 143 J. Average value of total impact energy at -20°C was lowered to 107 J, and at -40°C it was around 59 J. Finally, at -60°C the mean value of total impact energy was around 32 J.

As previously mentioned, temperature effect on total impact energy values was most prominent for test specimens with V-2 notch in the WM. At room temperature, total impact energy mean values was 156 J and at 0°C it was 111 J. Further decrease in temperature resulted in mean total impact energy value of 82 J for -20°C test temperature and 45 J for -40°C. Finally, at -60°C the mean value was around 29 J.

Annex D from standard SRPS EN ISO 148-1:2016, /16/, defines four criteria that can be used to determine the transition temperature. The most commonly used is the 27 J criterion, i.e. temperature at which the impact energy is equal to 27 J. Values of transition temperatures for all three welded joint regions are given in table 7.

Table 7. Transition temperatures for a welded joint

Notch location	Transition temperature, Tt, °C, at 27J
BM	-70.2.
HAZ	-65.5
WM	-61.6

Transition temperature is determined using the absorbed impact energy (KV) - temperature (T) curve, as shown in Fig. 18 for the BM, WM and HAZ.

Crack propagation energy share for BM specimens at room temperature is around 73% of total impact energy. This share decreases with the temperature, and is 59% at 0°C, 53% at -20°C, around 28% at -40°C and only 24% of total impact energy at -60°C.

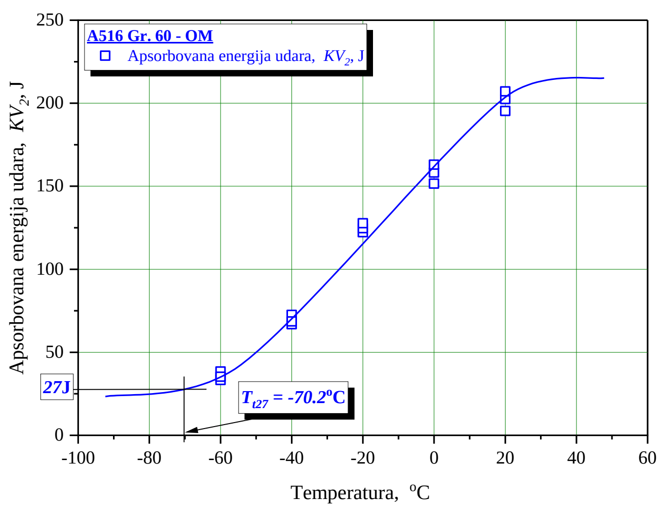

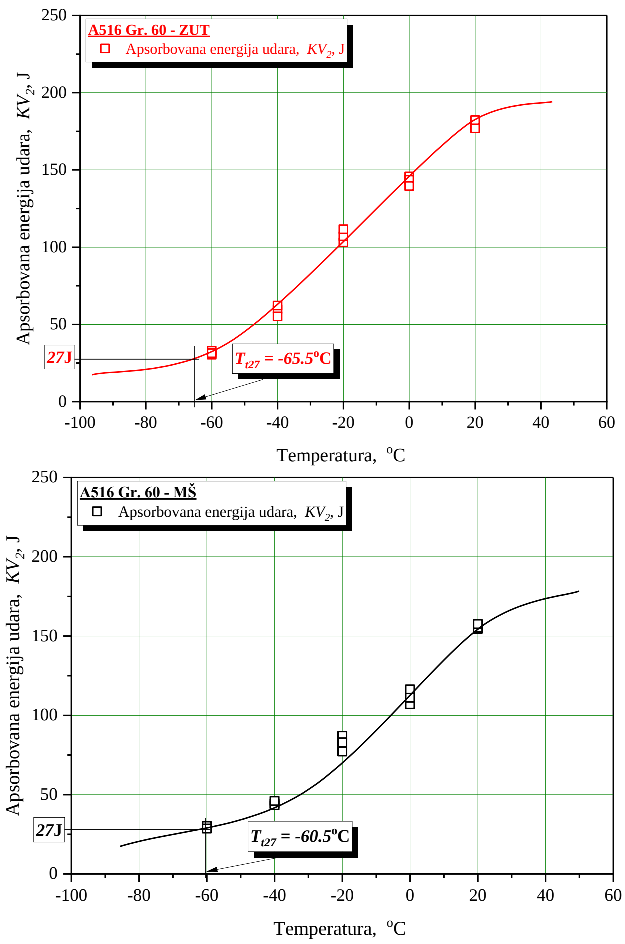

Figure 15. Total impact energy vs. temeprature (BM, HAZ, WM)

In the case of the HAZ, crack propagation energy share at room temperature is around 67% of total impact energy. This decreases to 54% for 0 °C, and continues to decrease at lower temperatures. At -20°C, crack propagation energy share is 51%, at -40°C it is around 24% and at -60°C it represents 13% of total impact energy.

As for specimens with the notch in the WM, room temperature tests had shown that the crack propagation energy share is around 58% of total impact energy, whereas at 0°C it is 48%. At -20°C test temperature, this share is around 40%, at -40°C it is 22%, and at -60°C it decreases to 11% of total impact energy.

CONCLUSIONS

The goal of this paper was to determine the behaviour of A516 Gr. 60 steel under impact load, for each welded joint zone (BM, HAZ and WM) tested at different temperatures,

Based on the obtained results, it was concluded that the specimens with a notch in the BM metal had shown the best behaviour under impact load, with highest impact energy values, and biggest share of crack propagation energy. Specimens with the notch in the WM had the lowest values, but all of the obtained results were still acceptable for each welded joint region, even at temperatures as low as -60°C. This was further confirmed after determining the transition temperatures for each welded joint region, all of which were below -60°C.

REFERENCES

1. Jovanović, M., Čamagić, I., Sedmak, S., Sedmak, A., Burzić, Z., (2022) The Effect of Material Heterogeneity and Temperature on Impact Toughness and Fracture Resistance of SA-387 Gr.91 welded joints. Materials 15,1854. DOI: 10.3390 /ma15051854
2. Jovanović, M., Čamagić, I., Sedmak, S., Sedmak, A., Burzić, Z., (2022) Effect of material heterogeneity and testing temperature on fatigue behaviour of Cr-Mo steel welded joints, Engineering Failure Analysis 141, 106542, DOI:10.1016/j.engfailanal.2022.106542.
3. Vojvodic-Tuma, J., Sedmak, A., (2004) Analysis of the unstable fracture behaviour of a high strength low alloy steel weldment, Engineering Fracture Mechanics, 71(9–10), 1435-1451, DOI: 10.1016/S0013-7944(03)00166-8
4. Mastilović, S., Djordjević, B., Sedmak, A., Kirin, S., (2023) Size effect assessment of K_{Jc} experimental data using the two-step-scaling method, Structural Integrity and Life, 23(2,) 105–110
5. Djordjevic, B., Mastilovic, A., Sedmak, A., Dimic, A., Kljajin, M., (2023) Ductile-to-brittle transition of ferritic steels: A historical sketch and some recent trends, Engineering Fracture Mechanics, 293, 109716. DOI: 10.1016/j.engfracmech.2023.109716.
6. Mastilovic, S., Djordjevic, B., Sedmak, A., Kirin, S., (2024) Data-driven prediction of fracture toughness size effect in ductile-to-brittle transition using Two-Step-Scaling procedure, Engineering Fracture Mechanics, 307, 110339. DOI: 10.1016/j.engfracmech.2024.110339
7. Đorđević, B., Sedmak, A., Petrovski, B., Sedmak, S.A., Radaković, Z., (2020) Load and Deformation Effects on Brittle Fracture of Ferritic Steel 20MnMoNi55 in Temperature Transition Region, Structural Integrity and Life, 20(2), 184–189
8. https://sij.acroni.si/assets/Uploads/SIQUAL-catalogue.pdf
9. ASTM A516/A516M-10, "Standard Specification for Pressure Vessel Plates, Carbon Steel, for Moderate- and Lower-Temperature Service", 2015.
10. R. K., Nanstad, R. L. Swain, R. G. Berggren, (1990) "Influence of Thermal Conditioning Media on Charpy Specimen Test Temperature, Charpy Impact Test: Factors and Variable", ASTM STP 1072, ASTM, p. 195, 1990.
11. SRPS EN ISO 9016:2022. "Испитивање са разарањем заварених спојева металних материјала - Испитивање ударом - Постављање епрувета, оријентација зареза и испитивање", Институт за стандардизацију Србије, 2022.
12. EN ISO 14556:2023 Metallic materials - Charpy V-notch pendulum impact test - Instrumented test method
13. S. Sedmak, A. Radovć, V. Grabulov, (2002), The analysis of crack initiation / propagation energy ratio in steel at different temperatures, Structural Integrity and Life, Vol. 2(1-2) pp. 5-10
14. M. Jovanović, I. Čamagić, S.A. Sedmak, P. Živković, A. Sedmak, (2020) Crack initiation and propagation resistance of HSLA steel welded joint constituents", Structural integrity and life, 20(1), 11–14
15. M. Jovanović, I. Čamagić, A. Sedmak, Z. Burzić, S. Sedmak, P. Živković (2021), Analysis of SA 387 Gr. 91 welded joints crack resistance under static and impact load, Procedia Structural Integrity 31, pp. 38-34, DOI: 10.1016/j.prostr. 2021.03.008
16. EN ISO 148-1:2017 (Metallic materials - Charpy pendulum impact test - Part 1: Test method - ISO 148-1:2016)",